

Effect of milling time variation on TiTaVWCr HEA powder as nuclear material on microstructure and mechanical properties by a mechanical alloying method

by Sutrisna -

Submission date: 09-May-2023 06:24PM (UTC-0700)

Submission ID: 2089049934

File name: utrisna_2023_IOP_Conf._Ser._Earth_Environ._Sci._1151_012052.pdf (1.07M)

Word count: 3704

Character count: 18822

PAPER · OPEN ACCESS

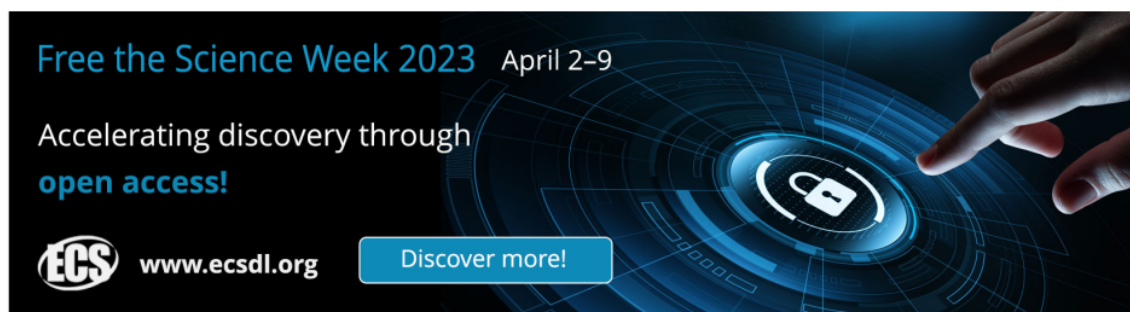
Effect of milling time variation on TiTaVWCr HEA powder as nuclear material on microstructure and mechanical properties by a mechanical alloying method

To cite this article: Sutrisna *et al* 2023 *IOP Conf. Ser.: Earth Environ. Sci.* **1151** 012052

View the [article online](#) for updates and enhancements.


You may also like

- 25 - Corrosion Behavior and Passive Film Characterization of Fe₅₀Mn₂₀Co₁₀Cr₂₀ Dual-Phase High-Entropy Alloy in Sulfuric Acid Solution
Yi-Sheng Lu, Che-Wei Lu, Yi-Ting Lin *et al*
- 6 - Deformation mechanism and tensile properties of nanocrystalline CoCrCuFeNi high-entropy alloy: a molecular dynamics simulation study
Anh-Son Tran
- 3 - Mobility of dislocations in FeNiCrCoCu high entropy alloys
Yixi Shen and Douglas E Spearot



Free the Science Week 2023 April 2-9

Accelerating discovery through
open access!

 www.ecsd.org [Discover more!](#)

The banner features a dark blue background with a futuristic, glowing interface. A hand is shown interacting with a circular element that contains a white padlock icon, symbolizing the unlocking of science through open access. The text is in white and light blue, providing clear information about the event and where to find more resources.

Effect of milling time variation on TiTaVWCr HEA powder as nuclear material on microstructure and mechanical properties by a mechanical alloying method

Sutrisna^{1*}, A B Prasetyo², R Kartikasari³ and I Aziz⁴

^{1,2,3}

^{1,2,3}Department of Mechanical Engineering, Institut Teknologi Nasional Yogyakarta, 55281, Indonesia

⁴Research Center for Accelerator Technology, National Research and Innovation Agency, Indonesia

sutrisna@itny.ac.id

Abstract. TiTaVWCr HEA alloy is a refractory material that is often used as nuclear material. This research uses powder material and milling using the mechanical alloy method. This research aimed to determine the microstructure and mechanical properties of the TiTaVWCr HEA alloy milling process for 4 h, 8 h, 16 h, and 24 h. Tests were carried out using XRD spectra and Secondary Electron Microstructure-Energy Dispersive Spectroscopy (SEM-EDS) to determine the characteristics of the material and its microstructure. The results showed that the HEA model with low milling (4 h and 8 h) microstructure distribution was not uniform, and there was agglomeration in certain areas. After milling was increased to 16 hours, the distribution of elements became uniform, but oxides appeared on Ti became in the formation of Ti-O. The hardness value shows that the longer the milling time, the higher the hardness. This phenomenon is related to the increase in grain dimension, and dislocation density.

12 Introduction

High entropy alloys (HEA) are alloys of materials with atomic concentrations of 5% to 35% and consist of a minimum of five elements in molar ratios or near [1]. HEA is one of the most promising structural materials in current developments for various industrial aerospace, automotive, and nuclear energy applications.[2][3]. In addition, HEA exhibits wonderful properties such as having high strength, high hardness value, good wear, and oxidation, and besides that, it is also resistant to corrosion, has high thermal stability, and has highly reputable mechanical properties [4][5]. Mixing HEA elements is a concept in the design of multi-component systems, and this concept will accelerate the development of new system alloys [6]. There are several techniques used in HEA fabrication, namely casting, arc-melting, sputtering, laser cladding, and mechanical alloying [7][8][9]. The melting temperature of HEA requires a very high temperature, hence it is made by melting and vacuum arc casting methods. Furthermore, the heat treatment process forms a homogeneous microstructure.

Recently, a mechanical alloying method has been developed for HEA production [10][11][12]. In this method, it is hoped that a smoother and more homogeneous mixture will be obtained.[13][14][15]. In



Content from this work may be used under the terms of the Creative Commons Attribution 3.0 licence. Any further distribution of this work must maintain attribution to the author(s) and the title of the work, journal citation and DOI.

Published under licence by IOP Publishing Ltd

addition, the mechanical alloying method can also combine and mix materials that have a high melting point with a low melting point [16][17]. Previous studies have reported by Oweis A et al [18] that nuclear fusion devices such as WTaTiVCr at high temperatures and having a high melting point exhibit high mechanical properties. In addition, this type of HEA has recently been investigated such as $Ti_xWTaVCr$ [19], $MoNbCrVTi$ [20], $NbMoTaWVCr$ [21], and $W_x(TaTiVCr)_{1-x}$ [22]. Their results showed that the HEA had high strength and hardness and a BCC crystal structure [23]. Likewise in the TiTaVWCr alloy, the BCC matrix occurs because of the Cr element which encourages the formation of the Laves phase. This happens because the element Cr has the smallest radius [23]. At high temperatures, the refractory HEA microstructure can affect the mechanical properties that it can increase strength, while at room temperature, it decreases. [24]

In this study, the materials used for the HEA refractory alloy were powder elements Ti, Ta, V, W, and Cr using the mechanical alloy method and thoroughly characterized. This study aims to study the effect of variations in milling time 4 h, 8 h, 16 h, and 24 h on the mechanical properties and microstructure after sintering at 1450°C.

2. Methodology

In this study, a powder material consisting of Ti, Ta, V, W, and Cr elements was used. These elements have particle sizes between 1 - 50 microns and purity above 99.5%. The chemical composition is the same for all elements. The method used in this research is to mix the elements first with the same percentage. After these elements were mixed, they were milled using a mechanical alloy method for 4 h, 8 h, 16 h, and 24 h. The milling process uses a planetary ball mill machine with a rotation speed of 300 rpm and the ratio between balls and powders is 10:1. During the milling process to prevent agglomeration, stearic acid was given as a process control agent.

Furthermore, the powder that has been milled is compacted with a pressure of 5 tons within 5 seconds to become a green compact. Then the compacted green compact was sintered at 1450°C and held for 1 hour. The XRD spectrum test was used to characterize the phase of the powder, while SEM-EDS was used to determine the microstructure and composition. Furthermore, the Vickers method was used to measure the hardness value using a 1 kg load held for 15 seconds, while the Archimedes method was used to determine the relative density.

9

3. Results and discussion

3.1. Characterization of Powders

Figure 1 shows the change in characteristic of powder using XRD spectrum analysis on mixed powders between Ta, Ti, V, W, and Cr after milling for 4 h, 8 h, 16 h, and 24 h. The un-milled powder showed very strong peak detection on some of these elements, in this case, the W element had the highest peak. This is because element W has the highest atomic mass compared to the other elements in this alloy [25]. In addition to showing strong peak reflections from these elements, there are also elements whose peaks overlap between Ta and Ti. This happens because the two elements have atomic radii that are close together [26].

After the milling time was increased from 4 h to 24 h there was a broadening of the peaks and the intensity decreased. This indicates that the milling process causes a decrease in crystal size. In addition, grain refinement and the occurrence of lattice strain are due to the grinding process. [27]. At the end of milling (24 h), BCC single-phase alloy powder structure was formed. [28], also due to the high-impact energy of the grinding medium and the long milling duration [29].

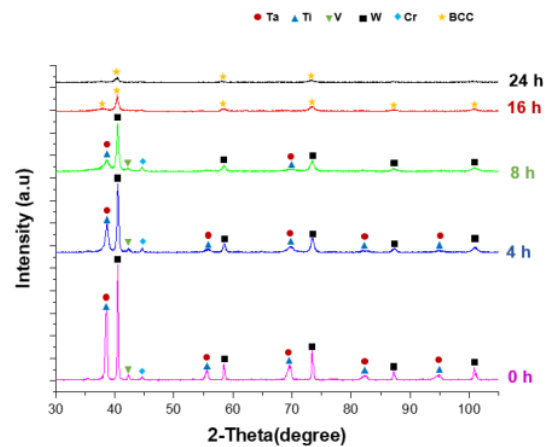


Figure 1. XRD spectra results of TiTaVWCr powder

3.2. Microstructural Characterization

3.2.1. *Microstructure Analysis* Microstructure of the TiTaVWCr equiatomic alloy with variations in grinding time for 4 h, 8 h, 16 h, and 24 h using the mechanical alloying method. The distribution of the structure is shown in Figure 2. At 4 hours of milling, the distribution of the structure was unequal in the HEA matrix; there was an agglomeration of Ti elements in certain areas. This shows that the milling is not complete and that diffusion occurs between the constituent elements. In addition, the solid solution has not been completely formed. The same thing happened to milling for 8 hours, as shown in Figures 2a and 2b, following the XRD test in Figure 1.

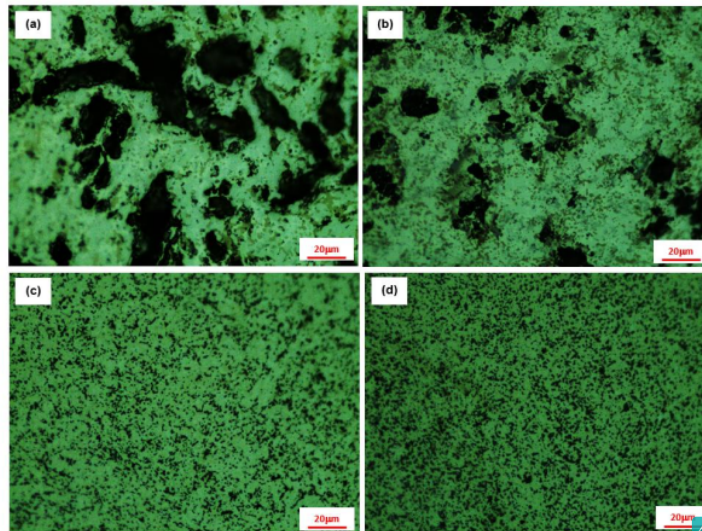


Figure 2. Results of optical microstructure with grinding time variation: (a). 4 h, (b). 8 h, (c). 16 h and (d). 24 h

3.2.2. After milling was increased to 16 hours. The distribution of the elements begins to be uniform, and a solid solution has occurred. However, element W still dominates the distribution and has a particle size of about 10 μm there are still significant differences in particle size. Increased milling time leads to even **20**ment distribution and smaller grains, and oxygen contamination. This is due to the grinding medium during the mechanical alloying process. [30]. In the final stage of milling, there is an even distribution of the oxide in the matrix. (Figure 2.d). In addition to the oxide dispersion, there is also elemental shrinkage and grain size refinement. As a result, the oxide particles that are produced when a Ti-rich precipitate is present form a core-shell, which reduces particle size and raises density. [31].

3.2.3. *EDS point Analysis* Figure 3 shows the EDS points of TiTaVWCr with variations in grinding time of 4 h, 8 h, 16 h, and 24 h. Milling for 4 h showed that the distribution of elements was incomplete that the distribution of elements was unequal and that some elements agglomerated in certain areas. Point 1 shows the TiTaVWCr HEA matrix with dominant tungsten other than Cr and Vanadium with a gray color, and from the milling and sintering process, there is still agglomeration in certain areas. High concentrations of Ti and O were also found at point 2 in Figure 2a. This shows that point 2 means that the oxide is rich-Ti, it also contains a small amount of element V. Furthermore, point 3 shows that Ti-oxide and elements V and Ta also appear, as well as what happened at milling of 8 h (Figure 3b).

The **15** presence of other elements appearing in the 8 h milling process indicates that the process has not completed the formation of a complete solid solution. After the milling time was increased to 16 h, a solid solution began to occur, and the distribution of elements spread evenly. At the end of **248** of milling (see Figure 3d) that the distribution of the elements is equal and a solid solution is formed. The distribution of elements is even between the HEA matrix and the other elements. The presence of oxides in the microstructure facilitates the formation of Ti oxide. The high oxide content in Ti can cause unwanted phase deposition during the sintering process. The deposition of this phase causes microstructure segregation [17].

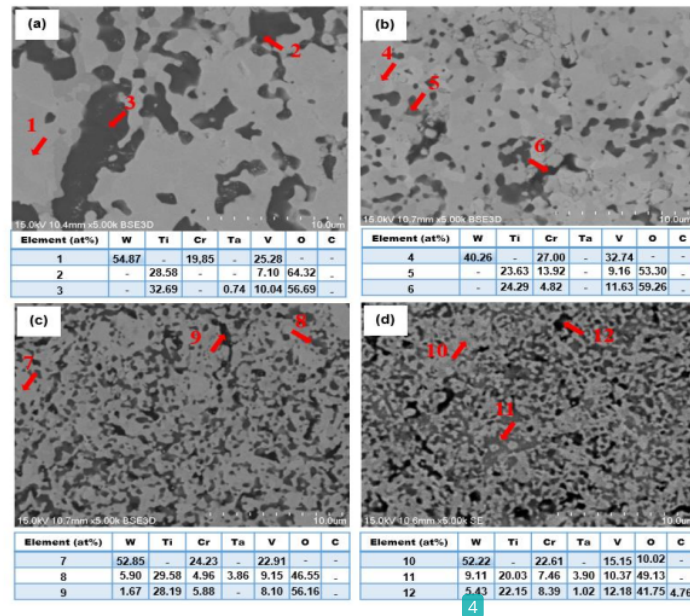


Figure 3. EDS images of the TiTaVWCr at grinding time of (a). 4 h, (b). 8 h, (c). 16 h and (d). 24 h

3.2.4. EDS Mapping Analysis The results of mapping the TaTiVWCr alloy at a milling time of 24 h are shown in Figure 4. This was done to determine the composition of each element. In this figure, the distribution of each element is clearly visible. On the element Ti, the oxide is also clearly visible. This indicates that the Ti-rich oxide can be easily formed by mechanical alloys with long milling times and high-temperature sintering[32][33]. In addition, the uniform distribution of elements in HEA materials can be correlated with single-phase BCC solid solutions.

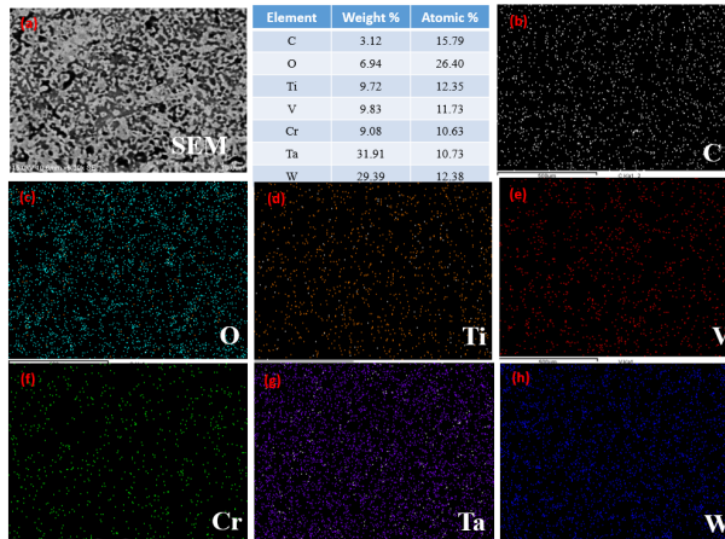


Figure 4. EDS mapping analysis of the TiTaVWCr after milling 24 h

3.2.5. Hardness Analysis Figure 5 shows the value of hardness that occurs during the milling process. It can be seen in the figure, that the longer the milling time, the higher the hardness value. At the beginning of milling (4 h), the hardness value was 432 HV. Furthermore, the milling time was increased to 8 h, there was a change in the hardness value that increased but was not significant (approximately 13%). This is correlated with the observation of the microstructure in Figure 2, that the distribution of the elements is not equally distributed, and there is no complete solid solution.

After the milling time was increased to 16 h, there was a very significant increase in the hardness value (about 58%). This increase in hardness value is caused by the composition of the elements that have been equally distributed and a solid solution formation. At the end of milling for 24 h, the hardness value also increased to 1306 HV, apart from the uniform elements distribution and the solid solution formation, oxides and carbon also appear as a result of the sintering process at high temperatures (1450°). As for the sintering process, in addition to identifying an increase in the hardness value, there is also an improvement in grain size and an increase in dislocation density and strain energy.

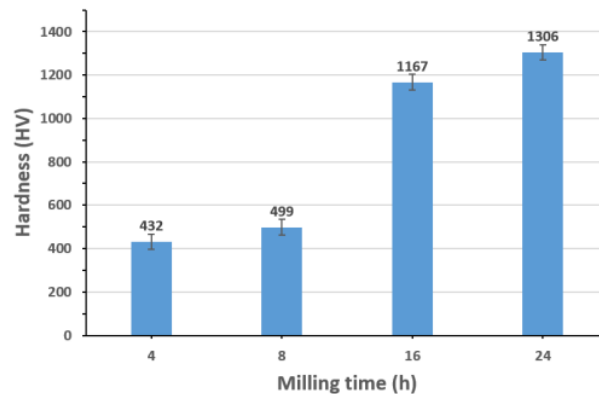


Figure 5. Vickers hardness value of the TiTaVWCr

The value of the relative density of TiTaVWCr is based on variations in milling time, the longer the milling time causes the density to be higher, as shown in Figure 6. Archimedes method was used in this measurement. At 4 h milling has a relative density of 83.75 gr/cm³; after the milling time is increased to 8 h, there is no significant change. This happens because, during the 4 h and 8 h milling process, the results are not perfect; there is still agglomeration in certain areas in the TiTaVWCr HEA alloy, as shown in Figure 2 (microstructure). Furthermore, after the milling was raised again until the end of milling (24 h), the relative density was very high (98.38 gr/cm³). It is closely related to the previous test (Figure 2c – d and Figure 4), that after milling for 24 h a solid solution occurs.

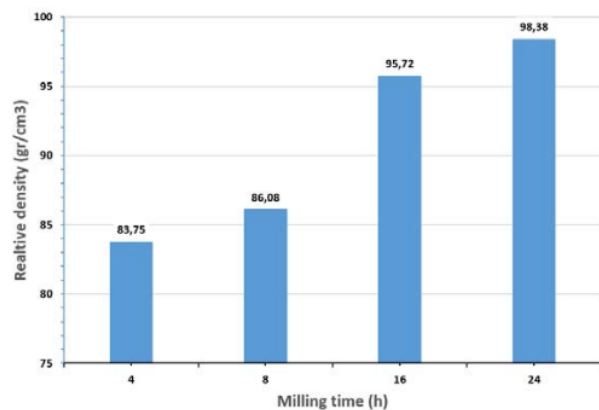


Figure 6. Relative density of the TiTaVWCr

4. Conclusions

Research has been carried out with variations in grinding time for 4 h, 8 h, 16 h, and 24 h on TiTaVWCr HEA equiatomic. The findings indicated that the solid solution phase of BCC was completely formed after 24 h milling, which was clearly visible on the XRD spectra test. The distribution of microstructure was equally distributed after 16 h, and at 24 h of milling time, oxides appeared which facilitated the Ti-oxide

formation. Phase deposition is formed due to the presence of high oxide content in Ti which causes the microstructure separation. Furthermore, the hardness value shows an increase with the length of milling time. This can be attributed to smaller grain size, dislocation density, and increased strain energy

References

- [1] Yeh J W, Chen S K, Lin S J, Gan J Y, Chin T S, Shun T T, Tsau C H, Chang S Y 2004 Nanostructured high-entropy alloys with multiple principal elements: Novel alloy design concepts and outcomes *Adv. Eng. Mater.* **6**
- [2] Xiang C, Han E, Zhang Z M, Fu H M, Wang J Q, Zhang H F, Hu G D 2019 Design of single-phase high-entropy alloys composed of low thermal neutron absorption cross-section elements for nuclear power plant application *Intermetallics* **104**
- [3] Geantă V, Voiculescu I, Ștefănoiu R, Chereches T, Zecheru T, Matache L & Rotariu A 2018 Dynamic impact behaviour of high entropy alloys used in the military domain In *IOP Conference Series: Materials Science and Engineering* **374**(1)1012041
- [4] Moravcikova-gouvea L, Moravcik I, Gouvea L, Hornik V, Kovacova Z, Kitzmantel M 2018 Synergic strengthening by oxide and coherent precipitate dispersions in high- entropy alloy prepared by powder metallurgy *Scr. Mater.* **157** 24–29
- [5] Senkov O N, Wilks G B, Scott J M, Miracle D B 2011 Mechanical properties of Nb₂₅Mo₂₅Ta₂₅W₂₅ and V₂₀Nb₂₀Mo₂₀Ta₂₀W₂₀ refractory high entropy alloys *Intermetallics* **19** 698–706
- [6] Zhang Y, Zhou Y J, Lin J P, Chen G L, Liaw P K 2008 Solid-solution phase formation rules for multi-component alloys *Adv. Eng. Mater.* **10** 534–538
- [7] Joo S, Kato H, Jang M J, Moon J, Kim E B, Hng S, Kim H S 2017 Structure and properties of ultra fine-grained CoCrFeMnNi high- entropy alloys produced by mechanical alloying and spark plasma sintering *J. Alloys Compd.* **698** 591–604
- [8] Chen Z, Chen W, Wu B, Cao X, Liu L, Fu Z 2015 Effects of Co and Ti on microstructure and mechanical behavior of Al_{0.75}FeNiCrCo high entropy alloy prepared by mechanical alloying and spark plasma sintering *Mater. Sci. Eng. A* 0–32
- [9] Ren B, Liu Z X, Shi L, Cai B & Wang M X 2011 Structure and properties of (AlCrMnMoNiZrB 0.1) N_x coatings prepared by reactive DC sputtering *Appl. Surf. Sci.* **257** 7172–7178
- [10] Suryanarayana C and Al-Aqeeli N 2013 Mechanically alloyed nanocomposites *Prog. Mater. Sci.* **58** 383–502
- [11] Vaidya M, Karati A, Marshal A, Pradeep K G & Murty B S 2019 Phase evolution and stability of nanocrystalline CoCrFeNi and CoCrFeMnNi high entropy alloys *J. Alloys Compd.* **770** 1004–1015
- [12] Shang X, Wang X, Chen S 2019 Effects of ball milling processing conditions and alloy components on the synthesis of Cu-Nb and Cu-Mo alloys *Materials (Basel)* **12** 1–9
- [13] Wang P, Cai H, Zhou S, Xu L 2017 Processing, microstructure and properties of Ni_{1.5}CoCuFeCr_{0.5-x}V_xhigh entropy alloys with carbon introduced from process control agent *J. Alloys Compd.* **695** 462–475
- [14] Materials H, Deng N, Zhou Z, Li J, Wu Y 2019 W – Cu composites with homogenous Cu – network structure prepared by spark plasma sintering using core – shell powders *International Journal of Refractory Metals* **82** 310–316
- [15] Matuła I, Zubko M, Dercz G 2020 Role of Sn as a process control agent on mechanical alloying behavior of nanocrystalline titanium based powders *Materials* **13** 2110
- [16] Tan J, Zhou Z J, Zhu X P, Guo S Q, Qu D D, Lei M K, Ge C C 2012 Evaluation of ultra-fine grained tungsten under transient high heat flux by high-intensity pulsed ion beam *Trans. Nonferrous Met. Soc. China (English Ed.)* **22** 1081–1085
- [17] Vaidya M, Karati A, Marshal A, Pradeep K G, Murty B S 2019 Phase evolution and stability of nanocrystalline CoCrFeNi and CoCrFeMnNi high entropy alloys *J. Alloys Compd.* **770** 1004–1015

- [18] Waseem O A and Ryu H J 2016 Tungsten-Based Composites for Nuclear Fusion Applications *Nucl. Mater. Perform* 139-162
- [19] Waseem O A, Lee J, Lee H M, Ryu H J 2018 The effect of Ti on the sintering and mechanical properties of refractory high-entropy alloy $\text{Ti}_{0.5}\text{W}_{0.5}\text{Ta}_{0.5}\text{V}_{0.5}\text{Cr}$ fabricated via spark plasma sintering for fusion plasma-facing materials *Mater. Chem. Phys.* **210** 87–94
- [20] Xiang C, Han E H, Zhang Z M, Fu H M, Wang J Q, Zhang H F, Hu G D 2019 Design of single-phase high-entropy alloys composed of low thermal neutron absorption cross-section elements for nuclear power plant application *Intermetallics* **104** 143–153
- [21] Long Y, Liang X, Su K, Peng H, Li X 2019 A fine-grained NbMoTaWVCr refractory high-entropy alloy with ultra-high strength: Microstructural evolution and mechanical properties *J. Alloys Compd* **780** 607–617
- [22] Yao X J, Shi X F, Wang Y P, Gan G Y, Tang B Y 2018 The mechanical properties of high entropy (-like) alloy $\text{W}_x(\text{TaTiVCr})_{1-x}$ via first-principles calculations *Fusion Eng. Des.* **137** 35–42
- [23] Materials H, Hamidi A G, Arabi H, Khaki J V 2019 International Journal of Refractory Metals Sintering of a nano-crystalline tungsten heavy alloy powder *Int. J. Refract. Metals Hard Mater.* **80** 204–209
- [24] Senkov O N, Senkova S V, Miracle D B, Woodward C 2013 Mechanical properties of low-density, refractory multi-principal element alloys of the Cr-Nb-Ti-V-Zr system *Mater. Sci. Eng. A.* **565** 51–62
- [25] Gregoire J M, Dale D, Van Dover R B 2011 A wavelet transform algorithm for peak detection and application to powder x-ray diffraction data *Rev. Sci. Instrum.* **82**
- [26] Gallhofer D and Lottermoser B G 2018 The influence of spectral interferences on critical element determination with portable X-ray fluorescence (pXRF) *Minerals* **8**
- [27] Wang C, Ji W, Fu Z 2014 Mechanical alloying and spark plasma sintering of CoCrFeNiMnAl high-entropy alloy *Advanced Powder Technology* **25**(4) 1334-1338
- [28] Ji W, Wang W, Wang H, Zhang J, Wang Y, Zhang F, Fu Z 2015 Alloying behavior and novel properties of CoCrFeNiMn high-entropy alloy fabricated by mechanical alloying and spark plasma sintering *Intermetallics* **56** 24–27
- [29] Vaidya M, Karati A, Marshal A, Pradeep K G, Murty B S 2019 Phase evolution and stability of nanocrystalline CoCrFeNi and CoCrFeMnNi high entropy alloys *J. Alloys Compd.* **770** 1004–1015
- [30] Xie Y, Zhou D, Luo Y, Xia T, Zeng W, Li C, Wang J, Liang J, Zhang D 2019 Fabrication of CoCrFeNiMn high entropy alloy matrix composites by thermomechanical consolidation of a mechanically milled powder *Mater. Charact.* **148** 307–316
- [31] London A J, Lozano-Perez S, Santra S, Amirthapandian S, Panigrahi B K, Sundar C S, Grovenor C R M, 2014 Comparison of atom probe tomography and transmission electron microscopy analysis of oxide dispersion strengthened steels *J. Phys. Conf. Ser.* **522**
- [32] Laurent-Brocq M, Goujon P A, Monnier J, Villeroy B, Perrière L, Pirès R, Garcin G 2019 Microstructure and mechanical properties of a CoCrFeMnNi high entropy alloy processed by milling and spark plasma sintering *J. Alloys Compd.* **780** 856–865
- [33] Gwalani B, Pohan R M, Lee J, Lee B, Banerjee R, Ryu H J, Hong S H 2018 High-entropy alloy strengthened by in situ formation of entropy-stabilized nano-dispersoids *Sci. Rep.* **8** 1–9

Acknowledgements

The author expresses his deepest gratitude to Institut Teknologi Nasional Yogyakarta for funding research and international conference, and Laboratory at Research Center for Accelerator Technology National Research and Innovation Agency Yogyakarta Indonesia provides facilities for research.

Effect of milling time variation on TiTaVWCr HEA powder as nuclear material on microstructure and mechanical properties by a mechanical alloying method

ORIGINALITY REPORT

16%

SIMILARITY INDEX

12%

INTERNET SOURCES

13%

PUBLICATIONS

4%

STUDENT PAPERS

PRIMARY SOURCES

- | | | |
|---|--|----|
| 1 | umpir.ump.edu.my
Internet Source | 2% |
| 2 | Suprianto, Chun-Liang Chen. "Study of (Ni,Cr) pre-milling for synthesis of CoFe(NiCr)Mn high entropy alloy by mechanical alloying", <i>Materials Science and Engineering: A</i> , 2021
Publication | 2% |
| 3 | Z M Chen, M Mrovec, P Gumbsch. " Atomistic aspects of $\langle 111 \rangle$ screw dislocation behavior in α -iron and the derivation of microscopic yield criterion ", <i>Modelling and Simulation in Materials Science and Engineering</i> , 2013
Publication | 1% |
| 4 | pure.rug.nl
Internet Source | 1% |
| 5 | Hamid Alihosseini, Kamran Dehghani. "Analysis of Particle Distribution in Milled Al-Based Composites Reinforced by B4C | 1% |

Nanoparticles", Journal of Materials Engineering and Performance, 2017

Publication

6

Anh-Son Tran. "Deformation mechanism and tensile properties of nanocrystalline CoCrCuFeNi high-entropy alloy: a molecular dynamics simulation study", Physica Scripta, 2021

Publication

1 %

7

Xiao Yang, Hongxia Zhang, Buyun Cheng, Yongquan Liu, Zhifeng Yan, Peng Dong, Wenxian Wang. "Microstructural, Microhardness and tribological analysis of cooling-assisted friction stir processing of high-entropy alloy particles reinforced aluminum alloy surface composites", Surface Topography: Metrology and Properties, 2020

Publication

1 %

8

centaur.reading.ac.uk

Internet Source

1 %

9

rd.springer.com

Internet Source

1 %

10

"Spark Plasma Sintering of Materials", Springer Science and Business Media LLC, 2019

Publication

<1 %

- | | | |
|----|--|------|
| 11 | Wang, Pei, Hongnian Cai, Shimeng Zhou, and Lingyu Xu. "Processing, microstructure and properties of Ni _{1.5} CoCuFeCr _{0.5-x} V _x high entropy alloys with carbon introduced from process control agent", Journal of Alloys and Compounds, 2017.
Publication | <1 % |
| 12 | dergipark.org.tr
Internet Source | <1 % |
| 13 | riaa.uaem.mx
Internet Source | <1 % |
| 14 | Krishanu Biswas, Nilesh Prakash Gurao, Tanmoy Maiti, Rajiv S. Mishra. "High Entropy Materials", Springer Science and Business Media LLC, 2022
Publication | <1 % |
| 15 | etheses.whiterose.ac.uk
Internet Source | <1 % |
| 16 | hdl.handle.net
Internet Source | <1 % |
| 17 | jtm.itp.ac.id
Internet Source | <1 % |
| 18 | "TMS 2018 147th Annual Meeting & Exhibition Supplemental Proceedings", Springer Nature, 2018
Publication | <1 % |

19 Shasha Lv, Yufei Zu, Guoqing Chen, Xuesong Fu, Wenlong Zhou. "An ultra-high strength CrMoNbWTi-C high entropy alloy co-strengthened by dispersed refractory IM and UHTC phases", Journal of Alloys and Compounds, 2019
Publication

20 dspace.vutbr.cz
Internet Source

21 link.springer.com
Internet Source

22 mdpi-res.com
Internet Source

23 mdpi.com
Internet Source

24 worldwidescience.org
Internet Source

25 www.nature.com
Internet Source

26 www.selleckchem.com
Internet Source

27 www.tandfonline.com
Internet Source

28 Cheenepalli Nagarjuna, Ashutosh Sharma, Kwan Lee, Soon-Jik Hong, Byungmin Ahn.

"Microstructure, mechanical and tribological properties of oxide dispersion strengthened CoCrFeMnNi high-entropy alloys fabricated by powder metallurgy", Journal of Materials Research and Technology, 2023

Publication

Exclude quotes Off

Exclude matches Off

Exclude bibliography On